Detection of Silicone in Lymph Node Biopsy Specimens by Near-Infrared Raman Spectroscopy

CHRISTOPHER J. FRANK, RICHARD L. McCREERY,* DOUGLAS C. B. REDD, and TED S. GANSLER

Department of Chemistry, The Ohio State University, 120 West 18th Ave., Columbus, Ohio 43210 (C.J.F., R.L.M.); and Department of Radiology (D.C.B.R.) and Department of Pathology (T.S.G.), Emory University School of Medicine, 1364 Clifton Road, N.E., Atlanta, Georgia 30332

Near-infrared Raman spectroscopy with a 782-nm cw laser was used to examine lymph node biopsy specimens from women with ruptured breast implants containing silicone gel. For reduction of fluorescence and sample radiation damage, a low-power (30 mW) Ti : sapphire laser, single-stage spectrograph, and CCD detector were employed. Silicone Raman features were clearly visible in lymph node tissue of patients with leaking implants, and the spectra were easily distinguished from those of normal lymph node tissue. The technique has promise for medical diagnostic purposes, and may be amenable to *in vivo* analysis with adaptation to a fiber-optic probe.

Index Headings: **Raman spectroscopy; Near infrared; Silicone; Breast implants.**

INTRODUCTION

In April of 1992, the Food and Drug Administration (FDA) restricted the use of silicone gel breast implants, citing lack of adequate information on the health risks associated with such implants. The highly publicized but still uncertain health risks of silicone leakage from implants prompted the recommendation by the FDA General and Plastic Surgery Devices Panel to restrict use of silicone implants. There is currently no commonly used diagnostic technique for confirming the presence of silicone in human tissues, either in biopsy samples or *in vivo*. Such a technique should be selective, sensitive, nondestructive, and minimally invasive.

Raman spectroscopy can be useful as a diagnostic or analytical technique in medicine since it provides a structural probe for components in biological material.[1-4] Raman spectroscopic investigations of biological materials have been hampered by fluorescence interference which often overwhelms the weak Raman scattering from these materials. Our laboratory has considered the use of near-infrared (NIR) Raman spectroscopy with diode lasers and charge-coupled device (CCD) detectors in order to reduce fluorescence interference.[5,6] Operation at 782 or 830 nm results in substantially reduced fluorescence, compared to excitation at 514.5 nm. Furthermore, CCD detectors are usually shot-noise limited when used with 782-nm lasers, yielding a high signal-to-noise (S/N) ratio at relatively low laser power (typically 10–30 mW, 100–300 W/cm^2, at the sample). Although FT-Raman with 1064-nm lasers further reduces fluorescence interference, the high laser powers often required frequently damage biological tissue.[7,8] NIR Raman spectroscopy with a pulsed Nd:YAG/dye laser and CCD detector has been successfully applied to human aorta tissue.[1,2] However, a 10-Hz pulsed Nd:YAG laser produces peak powers of ~200 kW for 20 mW average power (or ~10 MW/cm^2 for a typical spot size), thus raising the prospect of greater sample damage in comparison to that from a 20 mW cw laser. Thus, the use of NIR Raman with an efficient single spectrograph, a 782-nm cw laser, and a CCD detector permits Raman spectral acquisition with good sensitivity, but with minimal sample radiation damage.

Reconstruction or augmentation of the female breast has commonly made use of silicone bag-gel prostheses. A possible consequence of their use is rupture with leakage of silicone into the surrounding breast tissue and lymphatic drainage channels. In the post-mastectomy patient who has undergone surgical breast reconstruction following the removal of the cancerous breast, the discovery of enlarged axillary lymph nodes is clinically worrisome, as this condition may indicate the presence of recurrent (metastatic) disease. Alternatively, in those patients with silicone breast implants, this condition may also be due to infiltration of lymph nodal tissue by silicone gel secondary to prosthesis rupture. The ability to detect the presence of polydimethylsiloxane gel within lymph nodes (silicone lymphadenopathy) in these patients is clinically significant since the presence of silicone can only be indirectly inferred by light microscopy at the present time. Abraham and Etz[9] have reported the use of a laser Raman microprobe for detection of silicone elastomer particles in lymph nodes. The 60-μm silicone particles detected in their study were fragments which had migrated from a finger joint prosthesis. In the current report, the analytical technique of NIR Raman spectroscopy is utilized to study surgically excised axillary lymph node tissues. The ability to detect spectral

Received 19 October 1992.
* Author to whom correspondence should be sent.

0003-7028/93/4704-0387$2.00/0

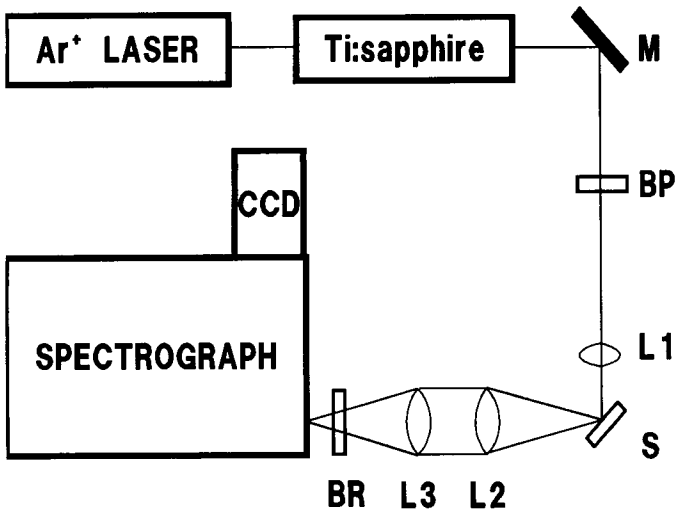

FIG. 1. Diagram of system components. **L1** is a focusing lens, **L2** is a 50-mm $f/1.4$ camera lens, and **L3** is a 25-cm $f/5$ biconvex lens. **BP** is an interference bandpass filter; **BR** is comprised of two holographic band-rejection filters. **M** is a mirror and **S** is the sample. The spectrometer and lasers are described in the text.

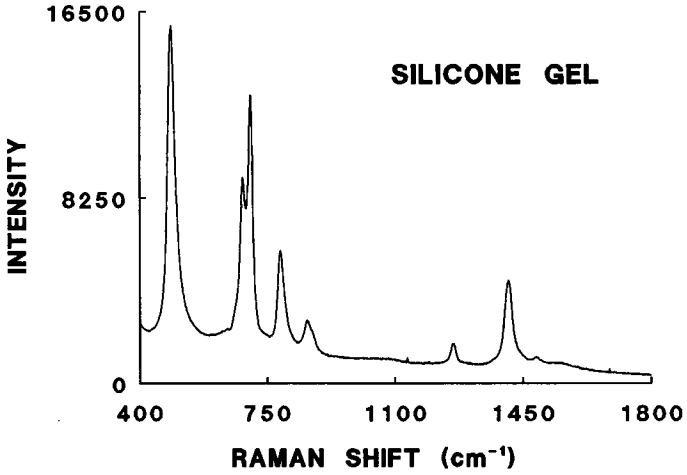

FIG. 2. Spectrum of silicone gel obtained with the Raman system in Fig. 1. Laser power was 30 mW (782 nm) at the sample with the use of a 50-μm entrance slit and 60-s CCD integration time.

features of polydimethylsiloxane in samples of both formalin-fixed tissue as well as those embedded in paraffin blocks is demonstrated. These results suggest that NIR Raman spectroscopy may find application in monitoring certain clinical conditions.

EXPERIMENTAL

The single-stage spectrograph was an Instruments SA HR640 (Metuchen, NJ) with a classically ruled grating of 300 lines/mm (blazed at 1.0 μm), resulting in a dispersion of 4.8 nm/mm at the focal plane. A Photometrics (Tucson, AZ) CCD detector (EEV CCD 05-10) with 296 × 1152 pixels (each 22.5 μm wide) was utilized to give an active detector area of 0.66 cm × 2.59 cm. All spectra were collected by binning the CCD in the vertical direction (short axis) to give 1152 resolution elements. The CCD was operated at −110°C in all cases and was controlled by a personal computer (PC) with CCD 9000 software. Additionally, the PC functioned to collect, store, and analyze the spectra. Laser excitation was provided by a tunable Coherent (Palo Alto, CA) Ti : sapphire laser (Model 890) pumped by a Coherent Innova 90 argon-ion laser. In this configuration with the mid-wavelength optics set and a 5-W pump, approximately 700 mW could be obtained from the Ti : sapphire laser at a wavelength of 782 nm. For the current experiments, the Ti : sapphire laser was operated at ~782 nm by tuning the laser to maximize transmission through an Omega (Brattleboro, VT) 782DF10 interference bandpass filter. The bandpass filter was necessary to remove nonresonant laser emissions. A diode laser may also be used for greater convenience, but the Ti : sapphire laser was used here for higher power and flexibility. By centering the spectrometer at a 1000-cm^{-1} Raman shift relative to the 782-nm laser line, we obtained spectral coverage at the focal plane of ~1800 cm^{-1} with 1.5 cm^{-1} per pixel. The spectrometer entrance slit was 1 cm high by 25–50 μm wide to give a theoretical bandpass of 1.6–3.3 cm^{-1}. The Raman shift range was calibrated with a Raman standard, indene[10] (Aldrich, Milwaukee, WI), each time the CCD was cooled or the grating was repositioned. Intensities are expressed as analog-to-digital (A/D) converter units with each A/D unit corresponding to approximately eight photoelectrons.

A diagram of the system components is given in Fig. 1. The collection optics were oriented at 90° with respect to the laser beam axis. Before impinging on the sample, the laser light (typically 30 mW) was focused to a ~200 μm spot (100 W/cm^2). The sample holder depended on sample type. Formalin-fixed tissue specimens were pinned to a foam support for sample alignment, while paraffin-embedded tissue blocks were affixed to a metal support. A three-axis positioner was used to align the sample with respect to the collection optics. The scattered light was collected by a 50-mm $f/1.4$ camera lens and then collimated. The collimated light was focused onto the entrance slit of the spectrograph by a 25-cm $f/5$ biconvex lens. Before the light entered the slit, the Rayleigh scattering was filtered by two Kaiser (Ann Arbor, MI) holographic band-rejection filters (HNF-785-1.0) and a 2-in. prototype band-rejection filter at 782 nm. Each filter had an optical density of ~4.0 at the 782-nm laser line and was angle tuned to provide the maximum Rayleigh rejection while maximizing the Stokes scattering intensities. Although the BR filters were not placed in the optimum location in the collimated region between **L2** and **L3**, their position closer to the slit improved the rejection of severely off-axis scattered light. All spectra are reported as collected, without smoothing or any correction for filter transmission, spectrograph transmission, or quantum efficiency of the CCD.

All tissue specimens were obtained following surgical excision from patients undergoing lymph node dissection related to surgery for lung neoplasm or for repeat breast reconstruction secondary to leaking silicone breast prosthesis. Surgical specimens were fixed in 10% paraformaldehyde, dehydrated in a graded series of alcohols, and washed in xylene prior to being embedded in paraffin. Ten-micron-thick sections were cut by microtome and stained with hematoxylin and eosin prior to light microscopy. All tissues were examined by a staff pa-

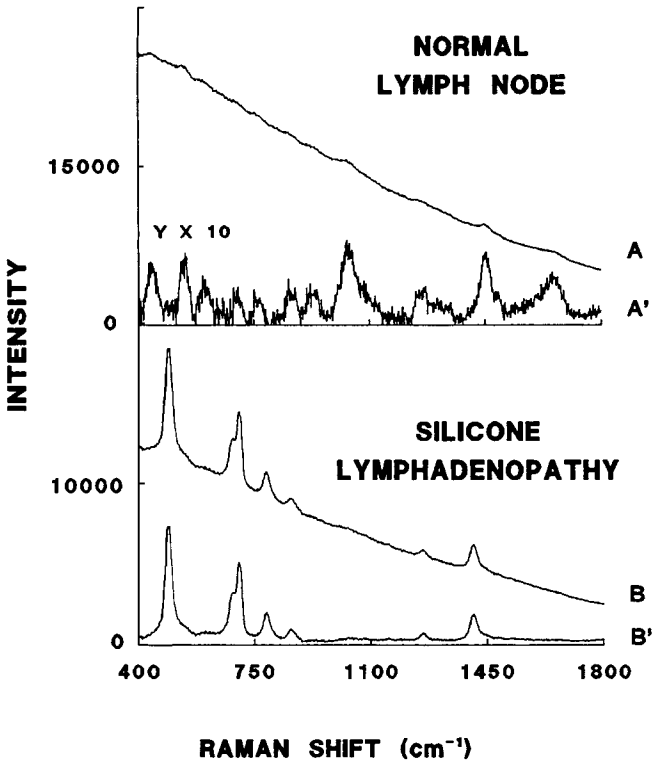

FIG. 3. Spectra of a normal axillary lymph node (spectrum *A*) and an axillary lymph node with silicone infiltration (spectrum *B*); both specimens are formalin-fixed. Spectra *A* and *B* were obtained with 30 mW (782 nm) of laser power with the use of 50-μm entrance slits and 60-s CCD integration time. Spectra *A'* and *B'* show the results of subtraction of the sloping backgrounds. Spectrum *B* demonstrates the detection of silicone in formalin-fixed axillary lymph nodes.

thologist at Emory University Hospital. Tissue specimens were obtained both following formalin fixation and following paraffin embedding and were studied spectroscopically with the operator (C.J.F.) blinded to the results of histopathological analysis. Normal and lymphadenopathy specimens were handled and prepared identically.

RESULTS AND DISCUSSION

A Raman spectrum of silicone gel aspirated from a surgically excised breast implant is shown in Fig. 2. The spectrum is similar to the Raman spectrum of polydimethylsiloxane rubber crosslinked by γ radiation reported by Maxfield and Shepherd.[11] The spectrum shows an excellent S/N ratio for a 60-second integration with 30 mW of laser power at the sample. A Raman spectral comparison of formalin-fixed normal lymph node and silicone lymphadenopathy is illustrated in Fig. 3. The top spectrum, *A*, shows a representative Raman spectrum of a normal lymph node removed from the right axilla with apparent fluorescence interference demonstrated even with 782-nm excitation. If the sloping fluorescence baseline is subtracted to yield spectrum *A'*, several Raman modes are apparent. The modes above 1000 cm^{-1} are due to lipid components in the tissue.[12] The features below 1000 cm^{-1} are due to intensity modulations induced by the holographic band-rejection filters. The location and intensity of the modulation features can be altered by changing the angle and placement

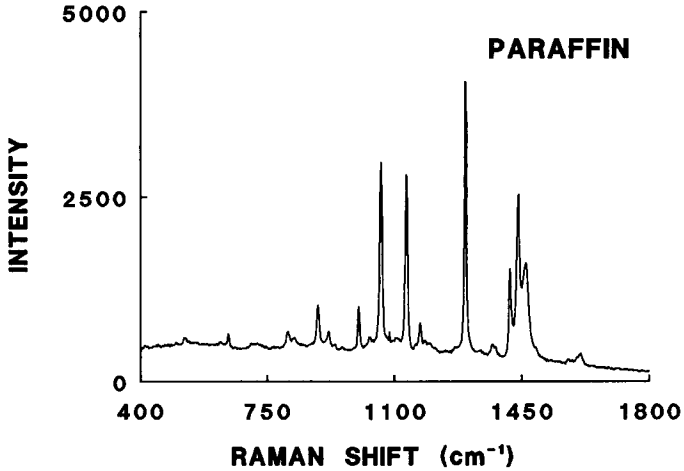

FIG. 4. Spectrum of embedding paraffin. Laser power was 30 mW (782 nm) with the use of 50-μm entrance slits and 60-s CCD integration time.

of the filters. Additionally, the features can be removed by appropriate spectral correction procedures which correct for filter function, spectrograph throughput, and quantum efficiency of the detector.[6] Spectrum *B* in Fig. 3 was obtained from lymph node tissue of a patient with a leaking silicone breast implant. Spectrum *B'* shows the result of subtracting the sloping fluorescence background, giving a Raman spectrum similar to the spectrum of silicone gel in Fig. 2. At least three locations of each of the tissue specimens in Fig. 3 were examined to ensure that the spectra were representative of the whole specimen. Additionally, several spectra were obtained at each location to make sure that the spectra were reproducible. No changes in spectra were observed with extended laser exposure.

Archival tissue specimens for histological evaluation are often preserved by embedding in paraffin. A Raman spectrum of a paraffin block is shown in Fig. 4. The above silicone lymphadenopathy specimen, as well as a normal axillary lymph node, was examined in the paraffin-fixed state. The top spectrum, *A*, in Fig. 5 shows a representative Raman spectrum of the normal axillary lymph node in paraffin. The modes from the paraffin matrix are the only observable bands atop the fluorescence background. After the sloping background was subtracted out, spectrum *A'* was obtained, which is similar to that of paraffin in Fig. 4. Filter intensity modulation features, visible in Fig. 3A, were significantly reduced by changing the filter angle with respect to the optical axis. The bottom spectrum of Fig. 5 shows silicone bands in an axillary lymph node which is preserved in paraffin. Spectrum *B* shows the paraffin modes along with two additional modes (marked with an asterisk) atop a fluorescence background. The two additional modes at 487 and 705 cm^{-1} are from silicone gel. After the background is subtracted, spectrum *B'* is similar to spectrum *A'* except for the two additional modes from silicone gel (marked with an asterisk). Both specimens in Fig. 5 were examined in several locations to ensure that the spectra reported were representative of the whole specimen.

The Raman spectra in the lower halves of Fig. 3 and Fig. 5 show that silicone lymphadenopathy of axillary

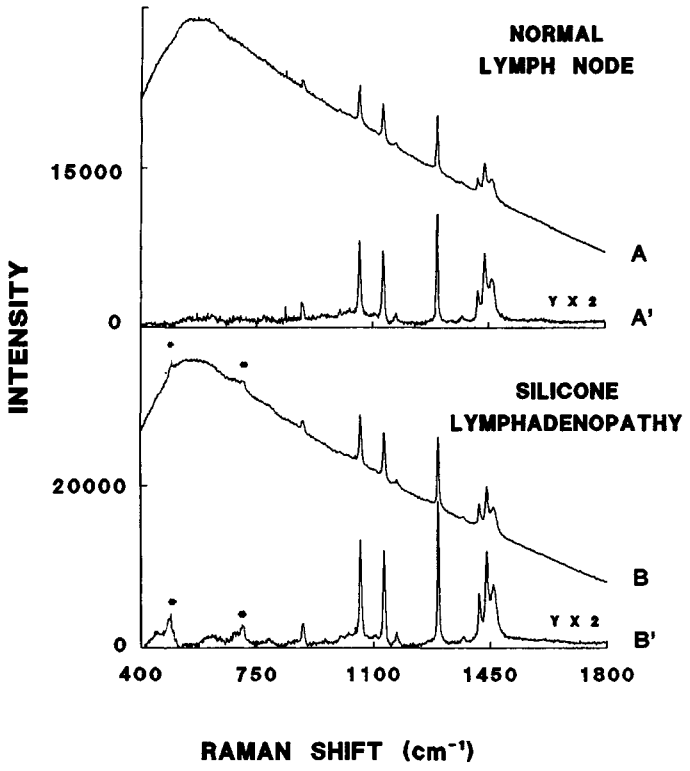

FIG. 5. Spectra of a normal axillary lymph node (spectrum *A*) and an axillary lymph node with silicone infiltration (spectrum *B*); both specimens were paraffin-fixed. Spectra *A* and *B* were obtained with 100 mW (782 nm) of laser power with the use of 25-μm entrance slits and 60-s CCD integration time. Spectra *A'* and *B'* show the results of subtraction of the sloping backgrounds. Spectrum *B* demonstrates the detection of silicone in paraffin-fixed axillary lymph nodes.

lymph node can be detected by Raman spectroscopy in formalin and paraffin-fixed biopsy samples. The analysis was performed on a relatively short time scale, one minute per sample. From the S/N ratio in the spectrum in Fig. 3, it is evident that shorter integrations can be used to provide a quicker analysis if necessary. Silicone lymphadenopathy was more easily detected in formalin-fixed specimens than in paraffin-fixed specimens. The clinical utility of Raman spectroscopy will depend on the reliability of detection and the complexity of the measurement. Although the instrument used here is very sensitive, it will need to be simplified for routine clinical applications. The use of compact spectrographs,[13] diode lasers, and thermoelectrically cooled detectors may sufficiently reduce instrumental complexity for routine use. A possibly important extension of the method would be adaptation to fiber-optic sampling. Not only could biopsy samples be examined quickly, but *in vivo* probes of living tissue would be feasible.

ACKNOWLEDGMENT

This work was supported by the Analytical and Surface Chemistry Division of the National Science Foundation.

1. J. J. Baraga, M. S. Feld, and R. P. Rava, Appl. Spectrosc. **46,** 187 (1992).
2. J. J. Baraga, M. S. Feld, and R. P. Rava, Proc. Natl. Acad. Sci. USA **89,** 3473 (1992).
3. V. R. Kodati, G. E. Tomasi, J. L. Turumin, and A. T. Tu, Appl. Spectrosc. **45,** 581 (1991).
4. Y. Ozaki, Appl. Spectrosc. Rev. **24,** 259 (1988).
5. J. M. Williamson, R. J. Bowling, and R. L. McCreery, Appl. Spectrosc. **43,** 372 (1989).
6. Y. Wang and R. L. McCreery, Anal. Chem. **61,** 2647 (1989).
7. T. Hirchfeld and D. B. Chase, Appl. Spectrosc. **40,** 133 (1986).
8. D. B. Chase, J. Am. Chem. Soc. **108,** 7485 (1986).
9. J. L. Abraham and E. S. Etz, Science **206,** 716 (1976).
10. P. J. Hendra and E. J. Loader, Chem. Ind. 718 (1968).
11. J. Maxfield and I. W. Shepherd, Chem. Phys. **2,** 433 (1973).
12. D. Redd, Z. C. Feng, K. T. Yue, and T. Gansler, paper to appear in Appl. Spectrosc. (June, 1993).
13. C. D. Newman, G. G. Bret, and R. L. McCreery, Appl. Spectrosc. **46,** 262 (1992).